Submitted to ApJ
Preprint typeset using LaTeX style emulateapj v. 11/12/01

PROBING THE REIONIZATION HISTORY OF THE UNIVERSE USING THE COSMIC MICROWAVE BACKGROUND POLARIZATION

Manoj Kaplinghat[1], Mike Chu[1], Zoltán Haiman[2,3,5], Gilbert P. Holder[4], Lloyd Knox[1] and Constantinos Skordis[1]

Submitted to ApJ

ABSTRACT

The recent discovery of a Gunn–Peterson (GP) trough in the spectrum of the redshift 6.28 SDSS quasar has raised the tantalizing possibility that we have detected the reionization of the universe. However, a neutral fraction (of hydrogen) as small as 0.1% is sufficient to cause the GP trough, hence its detection alone cannot rule out reionization at a much earlier epoch. The Cosmic Microwave Background (CMB) polarization anisotropy offers an alternative way to explore the dark age of the universe. We show that for most models constrained by the current CMB data and by the discovery of a GP trough (showing that reionization occurred at $z > 6.3$), MAP can detect the reionization signature in the polarization power spectrum. The expected 1-σ error on the measurement of the electron optical depth is around 0.03 with a weak dependence on the value of that optical depth. Such a constraint on the optical depth will allow MAP to achieve a 1-σ error on the amplitude of the primordial power spectrum of 6%. MAP with two years (Planck with one year) of observation can distinguish a model with 50% (6 %) partial ionization between redshifts of 6.3 and 20 from a model in which hydrogen was completely neutral at redshifts greater than 6.3. Planck will be able to distinguish between different reionization histories even when they imply the same optical depth to electron scattering for the CMB photons.

Subject headings: cosmic microwave background — cosmological parameters — cosmology: theory — galaxies: formation — early universe

1. INTRODUCTION

How and when the intergalactic medium (IGM) was reionized is one of the long outstanding questions in cosmology, likely holding many clues about the nature of the first generation of light sources and the end of the cosmological "Dark Age" (see Barkana & Loeb, 2001, for a review of our current understanding). The lack of strong HI absorption (the "Gunn–Peterson ", GP, trough) in the spectra of high redshift quasars has revealed that the intergalactic medium (IGM) is highly ionized between redshifts $0 \lesssim z \lesssim 6$. On the other hand, the lack of a strong damping by electron scattering of the first acoustic peak in the temperature anisotropy of the cosmic microwave background (CMB) radiation has shown that the universe was neutral between the redshifts $30 \lesssim z \lesssim 10^3$. Together these two sets of data imply that most hydrogen atoms in the universe were reionized during the redshift interval $6 \lesssim z \lesssim 30$.

The recent discovery by Becker et al. (2001) of the bright quasar SDSS 1030+0524 in the Sloan Digital Sky Survey (SDSS) at redshift $z = 6.28$ has, for the first time, revealed a full GP trough, i.e., a spectrum consistent with no flux at a substantial stretch of wavelength shortward of $(1 + z)\lambda_\alpha = 8850$Å. This discovery has raised the tantalizing possibility that we are detecting reionization occurring near redshift $z \sim 6.3$. The lack of any detectable flux indeed implies a strong lower limit $x_{\rm H} \gtrsim 0.01$ on the mean mass–weighted neutral fraction of the IGM at $z \sim 6$ (Fan et al., 2002; Pentericci et al., 2002). On the other hand, because of the large opacities of the hydrogen Lyman series, it is considerably difficult to push this method much further. In particular, in order to prove that we are probing into the neutral epoch, one would like to directly infer $x_{\rm H} \approx 1$. While in principle it is possible to infer this from the lack of any flux in a high enough S/N spectrum, in practice the required integration times are implausibly long.

In this paper, we discuss an alternative way of probing deeper into the dark ages. CMB polarization anisotropy at large angles is very sensitive to the optical depth to electron scattering for the CMB photons (Basko & Polnarev, 1980; Hogan et al., 1982; Zaldarriaga, 1997; Haiman & Knox, 1999, and references therein). In a model with no reionization, the polarization signal at large angles is negligible. However, CMB photons scattering in a reionized medium greatly enhance the polarization signal – making it very likely that such a signal (based on present CMB temperature anisotropy data and the GP trough) will be detected by the ongoing CMB satellite experiment MAP. We also show that Planck (and for large optical depths, MAP), will have the power to discriminate between different reionization histories even when they lead to the same optical depth.

The results from CMB polarization experiments will deepen our understanding of the physics of reionization. They will lead to better constraints on the models of reionization and, thereby, tell us much more about the first sources of light, and indeed, the first structures to form.

2. PROBES OF THE DARK AGE

Very little is known about the first sources and the reionization of the universe. Given the existence of the GP trough in the spectrum of the z=6.28 quasar, it is

[1]Department of Physics, 1 Shields Avenue, University of California, Davis, California 95616, USA
[2]Princeton University Observatory, Princeton, NJ 08544, USA
[3]Department of Astronomy, Columbia University, 550 West 120th Street, New York, NY 10027, USA
[4]Institute for Advanced Study, School of Natural Sciences, Olden Lane, Princeton, NJ 08540, USA
[5]Hubble Fellow

possible to argue on the basis of theoretical models and numerical simulations that reionization indeed occurred close to $z = 6.3$. The key ingredient in such arguments is that neutral fractions inferred from a sample of high redshift quasars show a rapid rise with redshift over the range $5.5 \lesssim z \lesssim 6$ (Songaila & Cowie, 2002). Semi–analytical methods (Haiman & Loeb, 1998, for example), as well as numerical simulations (Gnedin & Ostriker, 1998; Gnedin, 1999, for example) suggest that the initial phase of reionization proceeds very rapidly. During the "overlap" phase, when the individual HII regions of the ionizing sources percolate, the mean neutral fraction drops from unity by several orders of magnitude in a small fraction of the Hubble time. The reason for this rapidity is the fast timescale for the formation rate of the ionizing sources, which correspond to the high-σ peaks of the original density field. More recently, simulations of cosmological reionization (Cen & McDonald, 2002; Gendin, 2002; Fan et al., 2002), geared specifically to interpret the spectrum of SDSS 1030+0524, argued that the IGM is likely neutral at $z \gtrsim 6.5$.

While there may be a theoretical bias for reionization occurring close to $z = 6.3$, it is conceivable for reionization to last over a considerably longer redshift interval. This could be the case if the formation rate of the ionizing sources does not parallel the collapse of high-σ peaks, but is more gradual. Complete reionization could also be delayed for $\Delta z \gtrsim 1$ due to screening by minihalos with virial temperatures less than 10^4 K (Haiman et al., 2001; Barkana & Loeb, 2002). In addition, the decrease of the mean neutral fraction would be more gradual if the ionizing sources had a hard spectrum. Reionization by X–rays was considered recently by Oh (2001) and Venkatesan et al. (2001). In contrast to a picture in which discrete HII regions eventually overlap, in this case, the IGM is ionized uniformly and gradually throughout space.

An observational probe of the redshift–history of reionization would be invaluable in constraining such scenarios, and to securely establish when the Dark Age ended. Although detections of the hydrogen GP trough can not provide this type of constraint, a possibility may be to use corresponding absorption troughs caused by heavy elements in the high redshift IGM. Recently, Oh (2002) showed that if the IGM is uniformly enriched by metals to a level of $Z = 10^{-2} - 10^{-3}$ $Z_\odot$, then absorption by resonant lines of OI or SiII may be detectable. The success of this method depends on the presence of oxygen and silicon at these abundance levels, and also requires that metal enrichment precede hydrogen reionization.

An alternative method to probe the reionization history is to utilize the systematic changes in the profiles of Lyman alpha emission lines towards higher redshift. As argued in Haiman (2002), the increasing hydrogen IGM opacity towards higher redshift would make the emission lines appear systematically more asymmetric, and the apparent line-center systematically shifted towards longer wavelengths, as absorption in the IGM becomes increasingly more important, and eliminates the blue side of the line. Because of the intrinsically noisy Ly alpha line shapes, this method will require a survey that delivers a large sample of Ly alpha emitting galaxies (Rhoads & Malhotra, 2001).

Finally, it has been suggested that future radio telescopes could observe 21 cm emission or absorption from neutral hydrogen at the time of reionization (e.g., Hogan & Rees, 1979; Tozzi et al., 2000). This would provide a direct measure of the physical state of the neutral hydrogen and its evolution through the time of reionization. The detectability of the signal depends sensitively on the details of reionization and will require isolation of a signal that is much smaller than foreground contaminants. Recently, Carilli et al. (2002) also considered the radio equivalent of the GP trough. Unlike the Lyα case, the mean absorbtion by the neutral medium is about 1% at the redshifted 21 cm. While Carilli et al. (2002) considered the 21 cm absorbtion from large-scale structure using simulations, Furlanetto & Loeb (2002) and Iliev et al. (2002) have used semi-analytic methods to look at the observable features (in 21 cm) of minihalos and protogalactic disks. These studies argue that the 21 cm observations would yield robust information about the thermal history of collapsed structures and the ionizing background, sufficiently bright radio-loud quasars exist at $z_e > 6.3$.

As mentioned in the introduction, an alternative method to probe reionization is via the CMB anisotropy. The advantage of this method is that it probes the presence of free electrons, and can therefore detect $x_{\rm H} = 0.1$ and $x_{\rm H} = 10^{-3}$ with nearly equal sensitivity. Physically, the CMB and the GP trough therefore probe two different stages of reionization: the CMB is sensitive to the initial phase when $x_{\rm H}$ first decreases below unity, and free electrons appear, say, at redshift z_e. On the other hand, the (hydrogen) GP trough is sensitive to the end phase, or, going backward in cosmic time, when neutral hydrogen atoms first appear; say, $z_{\rm H}$. In currently popular theories, these two phases coincide to $\lesssim 10$ percent of the Hubble time, i.e. $z_e \approx z_{\rm H}$. However, as argued above, one can conceive alternative theories in which the two phases are separated by a large redshift interval, and $z_e \gg z_{\rm H}$.

Our goal in this paper is to quantify the power of CMB anisotropy to tell the difference between $z_e \gg z_{\rm H}$ and $z_e \approx z_{\rm H} \approx 6.3$, and more broadly, *whether there was substantial activity in the universe prior to z=6.3*. A similar question was addressed recently by Gnedin & Shandarin (2002), who consider the effects of reionization on maps of the temperature anisotropy. Our work is complementary, in that we focus on signatures of an extended period of partial reionization on the polarization anisotropy.

In addition to probing high–redshift structure formation, our calculations have importance for fundamental cosmology. In particular, the presence of free electrons damps the primary anisotropy, and results in a strong degeneracy between the amplitude of primordial fluctuations (A) and the electron scattering optical depth (τ). The quantity A is one of the most important parameters in inflationary cosmology, as it directly probes the inflaton potential. We show that the knowledge we gain about τ from MAP data will fix A with a precision of about 5%.

The $\tau - A$ degeneracy and the effect of CMB polarization on it has been studied before (Zaldarriaga et al., 1997; Wang et al., 1999; Eisenstein et al., 1999; Tegmark et al., 2000; Prunet et al., 2000; Venkatesan, 2002), using Fisher matrix methods. The resulting measures of τ and A have been shown to be powerful constraints on models of reionization (Venkatesan, 2000, 2002), and it has also

been shown that introducing some reasonable constraints on models of reionization can allow improved estimates of cosmological parameters. In previous work, the epoch of reionization has been treated as a sharp transition at a single redshift, leading to all information on reionization from CMB measurements encoded by a single number, τ. We show below that there is significantly more information in the large angle polarization anisotropy measurements. This will eventually allow more sophisticated tests of models of reionization.

3. REIONIZATION SIGNATURES IN THE CMB

Reionization affects the CMB anisotropy in a simple manner. On large angular scales, reionization has no effect, while on smaller scales it damps the anisotropy by a factor of $\exp(-2\tau)$. The division into large and small scales is dictated by the angle subtended by the horizon at reionization. The multipole moment this angular scale maps onto is given by $l_r = D_A(z(\eta_r))/\eta_r$, where η_r is the visibility function weighted conformal time (Hu & White, 1997) and $D_A(z)$ is the angular diameter distance to redshift z. The above assumes that the photons scattering off of the reionized electrons do not pick up additional anisotropy. While not strictly correct, this approximation is good for $\tau \lesssim 0.3$. The electron scattering optical depth is given by

$$\tau = \int_0^{z_e} dz \sigma_{\rm T} n_e(z) c \frac{dt}{dz}$$
$$\tau = 0.038 \omega_b h/\omega_m \left[\left(\Omega_\Lambda + \Omega_m \left(1+z_e\right)^3\right)^{1/2} - 1\right], \quad (1)$$

where $\sigma_{\rm T}$ is the Thompson cross section, n_e is the electron abundance, and $\omega_b \equiv \Omega_b h^2$ and $\omega_m \equiv \Omega_m h^2$ are the baryon and matter densities (respectively) scaled to the critical density today. Eq. (1) is correct for flat $w = -1$ models (Hu & White, 1997), and we have assumed complete ionization of H and ^{4}He to H^+ and $^4He^+$ respectively out to a redshift of z_e.

The effects of reionization on CMB polarization anisotropy are similar to that on the temperature anisotropy. At $l \gg l_r$, the polarization angular power spectra are suppressed by $\exp(-2\tau)$. However, in contrast to the temperature power spectrum, the effect at $l \lesssim l_r$ is quite dramatic (see Figure 2). Note that there is no analog of the Sachs-Wolfe (or the integrated Sachs-Wolfe) effect for polarization. All of the polarization signal is generated at the last scattering surface at $z \sim 1,000$ in the absence of reionization. Thus without reionization, the polarization power at small multipoles is negligible. In the reionized universe, the rescattering of photons in the presence of a large quadrupole temperature anisotropy results in a broad peak in polarization power at low l. For a detailed discussion of this "reionization bump", we refer the reader to Zaldarriaga (1997). Here we provide an overview.

We first note that since most of the optical depth to reionization is generated prior to the onset of curvature or dark energy domination, the reionization bump depends on curvature and dark energy only through their effect on D_A. The polarization anisotropy is sourced by the total quadrupole anisotropy – which for practical purposes is just the temperature quadrupole. The relevant quantity is the quadrupole at the reionization surface. The quadrupole produced at the last scattering surface (as the tight coupling breaks down) is small; however free-streaming after last scattering transfers power from the monopole to higher multipoles thus producing an appreciable quadrupole during reionization. The modes contributing to the reionization signal are $k \sim 2/\eta_r$ which become sub-horizon well after recombination. Thus the quadrupole on these scales does not depend on the baryon density. It does depend on the matter density when $\omega_m \lesssim 0.05$ since then there's significant radiation around when the relevant modes enter the horizon and the integrated Sachs-Wolfe effect will change the quadrupole. For the most part, the reionization bump is only sensitive to the electron optical depth and the amplitude of primordial potential fluctuations.

The arguments outlined above allow us to obtain the low-l E mode polarization anisotropy spectrum and its cross term with the temperature spectrum by simply scaling from a fiducial model. The temperature auto-correlation, polarization auto-correlation and the temperature-polarization cross-correlation spectra are denoted by C_{Tl}, C_{El} and C_{Cl} respectively. The E subscript refers to the E (electric or scalar) mode and the corresponding pseudo-scalar B mode is absent from scalar perturbation generated polarization anisotropy (Kamionkowski et al., 1997; Zaldarriaga & Seljak, 1997). In terms of $\mathcal{C}_{Xl} \equiv l(l+1)C_{Xl}/2\pi$ (where X stands for E,T or C), the scaling from the fiducial model (denoted by "$*$") is given by (Kaplinghat et al., 2002):

$$\mathcal{C}_{El'} = \mathcal{C}_{E_* l} \frac{(1-e^{-\tau})^2}{(1-e^{-\tau_*})^2} \left(\frac{\tau_*}{\tau}\right)^{(0.2-\tau_*/3)} \left(\frac{2}{l_{\rm pivot}}\right)^{n-1} \frac{A}{A_*},$$
$$\mathcal{C}_{Cl'} = \mathcal{C}_{C_* l} \frac{(1-e^{-\tau})}{(1-e^{-\tau_*})} \left(\frac{\tau_*}{\tau}\right)^{0.2} \left(\frac{2}{l_{\rm pivot}}\right)^{n-1} \frac{A}{A_*}, \quad (2)$$

where $l_{\rm pivot} \equiv (6000 \text{ Mpc } k_{\rm pivot})/\sqrt{\omega_m(1+z_{\rm ri})}$ and the initial potential power spectrum is taken to be of the form $k^3 P(k) = A\ (k/k_{\rm pivot})^{n-1}$ with $k_{\rm pivot} = 0.05$/Mpc. The angular diameter distance shifting is achieved through the relation $l' = l(l'_r/l_r)$ for $\mathcal{C}_{El}$ and $l' = l(l'_r + 0.5)/(l_r + 0.5)$ for $\mathcal{C}_{Cl}$.

The main features of the scaling are simple to elucidate. In the limit of small τ, the factor of $1 - \exp(-\tau)$ gives the fraction of scattered photons. The $\tau_\star/\tau$ factor is just a numerical fit which makes Eq. 2 more accurate. The dependence on the temperature quadrupole to generate the polarization anisotropy signal is clearly evident in the $n \neq 1$ pivot factor. The projection formula in l reflects the fact that most of the action during reionization happens close to the actual epoch of reionization (since the visibility function falls with increasing time). The above approximate scalings are good to about 10% around the peak of the "reionization bump" for $\tau \lesssim 0.3$. For our fiducial ("$*$") model we adopt a cosmology with $\tau = 0.15$, $\omega_b = 0.02$, $\omega_m = 0.16$ and $\Omega_\Lambda = 0.65$.

Although the process of reionization is expected to be spatially inhomogeneous, this should have little effect on the large scale polarization anisotropy discussed in the present study. The details of the typical patch sizes of reionized "bubbles", and their spatial correlations are not yet well–understood theoretically (Madau et al., 1999; Ciardi et al., 2000; Gnedin, 2000; Miralda-Escudé et al., 2000; Nakamoto et al., 2001). However, it appears likely that most of the ionizing radiation was provided by galaxies, (Haiman, 2001; Oh & Haiman, 2002, rather than quasars,

for example), and the typical patch sizes are expected to be $\mathcal{O}$(1 comoving Mpc). Inhomogeneities can remain significant above the typical patch size scale because of spatial correlations of the ionizing sources (Knox et al., 1998; Oh, 1999). However, these correlations fall off rapidly with increasing distance (approximately as $1/r^{1.8}$). For the large angle polarization features described here the relevant modes are $k \sim 2/\eta_r$; we do not expect correlations to significantly affect such horizon scale features (also see Gruzinov & Hu, 1998; Liu et al., 2001).

4. IONIZING RADIATION AND MAXIMUM OPTICAL DEPTH

CMB anisotropy is sensitive to both cosmological parameters and reionization history. As a result, any prior knowledge about reionization can, in principle, tighten cosmological constraints, and vice-versa. For the most part, we will adopt a conservative approach and obtain constraints without assuming any such *a priori* knowledge. In this section, however, we briefly consider simplified semi–analytical models of reionization, and how they can tighten constraints inferred from CMB data. Reionization and its dependence on cosmology has been studied more thoroughly by Venkatesan (2002) in the context of specific reionization models. Here we restrict our analysis to obtaining a theoretical *upper limit* to the reionization optical depth. In any cosmology with Gaussian seed density fluctuations, the amount of non–linear mass towards high redshifts declines exponentially, and hence a relatively robust upper limit can be derived.

In order to reionize the universe, the ionizing source must have (1) produced at least ~ 1 ionizing photon ($E >$ 13.6eV) per hydrogen atom, and (2) the rate of production of ionizing photons must be sufficient to balance recombinations, and keep the hydrogen ionized. Assuming a uniform gas distribution at the mean IGM density, the hydrogen recombination rate divided by the expansion rate is roughly equal to $(11/(1+z))^{1.5}$, which implies that recombinations are inevitably significant at $z \gtrsim 10$. We therefore focus on the second criterion above.

The ionizing photon production rate in the early universe depends on several factors: the rate at which gas is converted into new ionizing sources; the initial mass function (IMF) of the ionizing source population, the photon production rate per source (as a function of mass), and the fraction of ionizing photons escaping into the IGM. Here we make the following conservative assumptions. The rate of converting gas into new ionizing sources is given by the fraction of mass collapsed into dark matter halos with virial temperatures of $T > 10^4$K (computed using the formalism of Press & Schechter (1974); see discussion and justification in Haiman (2001)). We assume that all the gas in these halos turns into ionizing sources, and produces 10^4 ionizing photons per baryon. This is a conservative number; although massive ~ 1000 $M_\odot$ metal–free stars can produce upto ~ 100 times more ionizing photons (Tumlinson & Shull, 2000; Bromm et al., 2001), numerical simulations indicate that $\lesssim 1\%$ of the available baryons are expected to turn into ionizing sources (Abel et al., 2000). We further assume that all ionizing photons escape the source; in comparison, escape fractions of $\sim 10\%$ are measured in local starburst galaxies (Leitherer et al., 1995) (although larger escape fractions have been tentatively inferred for a sample of redshift $z \approx 3$ galaxies, Steidel et al. (2001)). Finally, in computing the global recombination rate, we assume a mean clumping factor for ionized hydrogen of $C_{\rm int} \equiv \langle n^2_{\rm HII}\rangle/\bar{n}^2_{\rm HII} = 20$; this is conservative in comparison with numerical simulations (Gnedin, 2000; Gnedin & Ostriker, 1997).

The above assumptions allow us to predict the maximum reionization redshift, and hence a maximum optical depth $\tau_{\rm max}$, given a cosmology. As an example, our formalism yields $z_{\rm max} = 20.6$ and $\tau_{\rm max} = 0.18$ for a flat cosmology with $\omega_m = 0.15$, $\omega_b = 0.02$ and $\sigma_8 = 1$. Note that this upper limit is significantly higher than the expected "ballpark" values in similar cosmologies (Haiman & Loeb, 1998; Gnedin & Ostriker, 1998), $z \sim 7-10$. We also reiterate that our result for $\tau_{\rm max}$ is relatively insensitive to our input assumptions, because of the steep decline in the collapsed mass fraction towards high redshifts. In our analysis of CMB anisotropy data in the next section, we will study the effects of including the constraint that the reionization optical depth not exceed $\tau_{\rm max}$.

5. IS THE POLARIZATION FEATURE DETECTABLE BY MAP?

In this section we examine how well MAP will be able to determine τ. This question has already been answered for particular models (Eisenstein et al., 1999; Tegmark et al., 2000; Prunet et al., 2000; Venkatesan, 2002). However, the answer depends on the choice of cosmological parameters, including τ. Here we calculate the *probability distribution* for $\sigma(\tau)$, the expected uncertainty in the measurement of τ, assuming flat adiabatic models of structure formation as constrained by current CMB and quasar spectral data.

Calculating $P(\sigma(\tau))$ is a three–step process. Step one is the generation of a Markov chain of locations in the parameter space with the remarkable property that the fraction of models in a given volume of parameter space is equal to the posterior probability in that region; i.e., a histogram of the frequency of occurence of parameter values in the chain ("histogramming the chain") gives the shape of the posterior probability distribution function (Christensen et al., 2001). We assume a flat cosmological model and take our (chain) parameters to be ω_b, ω_d, Ω_Λ, A, n, x (where $\tau = |x|$), four calibration parameters, and a parameter to account for the Boomerang beam size uncertainty (Netterfield et al., 2002). For this section, we assume instantaneous reionization. The data we use are from DASI (Halverson et al., 2002), Boomerang (Netterfield et al., 2002), DMR (Bennett et al., 1996) and Maxima (Lee et al., 2001). Generation of the chain requires as many likelihood evaluations as there are chain elements (in this case 300,000 evaluations). We use DASh (Kaplinghat et al., 2002) which rapidly and accurately calculates C_l and performs the likelihood calculation using the offset lognormal approximation of Bond et al. (2000).

Step two is the calculation, for each chain element, of "derived parameters" (parameters that are derived from the chain parameters). Our derived parameters include $z_{\rm ri}$, $\sigma_E(\tau)$ and $\sigma_C(\tau)$. The latter two are the errors expected on τ from MAP's measurement of C_l^E and C_l^C respectively. We calculate $z_{\rm ri}$ by inverting Eq. 1.

We calculate $\sigma_E(\tau)$ and $\sigma_C(\tau)$ by

$$\sigma_C^{-2}(\tau) = \sum_l \left(\frac{\partial C_{Cl}}{\partial \tau} / \Delta C_{Cl} \right)^2$$
$$\sigma_E^{-2}(\tau) = \sum_l \left(\frac{\partial C_{El}}{\partial \tau} / \Delta C_{El} \right)^2 \quad (3)$$

where (for low l) (Zaldarriaga et al., 1997)

$$(\Delta C_{El})^2 = 2 \frac{\left(C_{El} + w^{-1}\right)^2}{(2l+1) f_{\rm sky}}$$
$$(\Delta C_{Cl})^2 = \frac{C_{Cl}^2 + (C_{Tl} + w^{-1}/2)(C_{El} + w^{-1})}{(2l+1) f_{\rm sky}} \quad (4)$$

and $w = 2 \times 10^{14}$ is the expected weight–per–solid angle (for polarization measurements) from combining MAP's 90 GHz and 60 GHz channels for two years. In calculating our results throughout the paper, we set $f_{\rm sky} = 1$ (since $f_{\rm sky}$ is expected to be close to unity for the satellite experiments). Interested readers can scale our results to any value of $f_{\rm sky}$ using Eq. 4. We calculate C_{El} and C_{Cl} at each point in the chain using Eq. 2. The partial derivatives are calculated by finite differencing and are accurate to $\sim 10\%$ around the peak of the signal. Further, the derivatives are taken at fixed $A_\tau = A \exp(-2\tau)$ since this quantity will be well–determined by high l CMB measurements.

Step three is the histogramming of the chain, with addition of various prior constraints. In this case, the priors are tophats implemented by simply restricting the counting of models to those with $z_{\rm ri}$ in the desired range.

We have not included effects of foreground contamination because very little is known about polarized emission from foregrounds in the relevant frequency range. Tegmark et al. (2000) have tried to model our ignorance of the foregrounds and use the CMB maps to learn more about the foregrounds. The good news from their study is that foregrounds can be removed, but this results in larger error bars for the estimated cosmological parameters. With a "conservative" estimate for the amplitudes of foregrounds, Tegmark et al. (2000) showed that the expected error in τ could increase by a factor of about 2 relative to the expected error assuming no foregrounds. For this analysis they used all 5 MAP channels to fit the cosmological and their foreground model parameters jointly. However, the amplitude of the polarized foregrounds is unknown. If this amplitude is a factor of 10 larger (i.e., the power is a factor of 100 larger), then Tegmark et al. (2000) estimate that the error on τ goes up by a factor of about 10.

For simplicity, we assume MAP's 22, 30 and 40 GHz channels are used entirely for foreground removal, allowing the total weight of the 60 and 94 GHz channels to be used for the CMB. Also, foregrounds may significantly contaminate C_{Cl} but not C_{El}, or vice–versa and hence the existence of two different statistical channels to determine τ increases our chances. Note that the errors $\sigma_E(\tau)$ and $\sigma_C(\tau)$ are correlated and this must be taken into account if one were to combine them into a final error for τ.

We show the results of the exercise detailed in this section in Fig. 1. The four panels in the figure show contours of equal probability (1 and 2-σ) in the $\sigma_E(\tau)$ and $\sigma_C(\tau)$ vs. τ and z_e planes. We have plotted these contours for different priors on z_e. If reionization is indeed instantaneous, then the $6 < z_e < 7$ prior (solid contours) is the interesting case to study. However, as we stressed before, partial reionization is possible at redshifts $z_e > 6$, and hence we have included contours with more conservative priors: $6 < z_e < 10$ (dashed contours) and $6 < z_e$ (dotted contours).

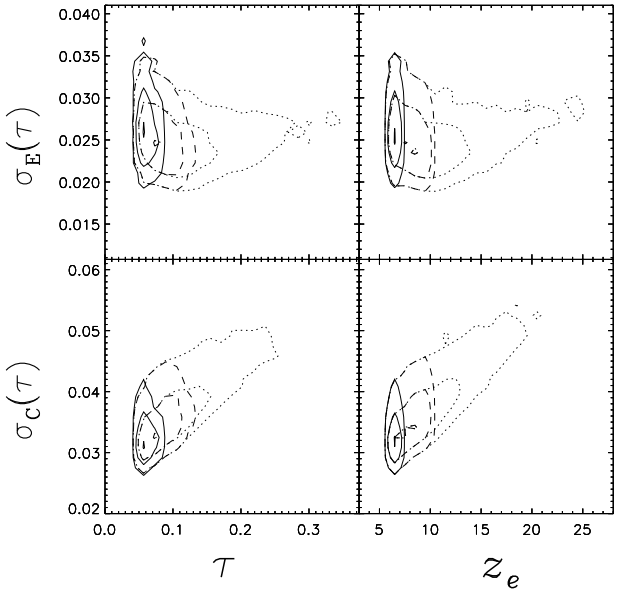

FIG. 1.— 1 and 2-σ joint probability contours of optical depth τ (or z_e) and the expected uncertainty with which MAP can measure τ in two years of operation. Measurements of τ using the E (EE) and the C (TE) channels are considered separately. The left panels show the τ, $\sigma_{E,C}(\tau)$ contours and the right panels show the z_e, $\sigma_{E,C}(\tau)$ contours. We have included three different priors on z_e. The dotted contours are for $z_e > 6$, the dashed contours are for $6 < z_e < 10$, and the solid contours are for $6 < z_e < 7$.

The result to take away from Figure 1 is that MAP will be able to determine τ to about 0.02 to 0.03 regardless of the value of τ. The lack of dependence of $\sigma_E(\tau)$ on τ is due to two reasons. First, at its peak $C_{El} \propto \tau$ (that this is approximately true can be ascertained from Eq. 2) and hence around peak power $\partial C_{El}/\partial\tau$ is approximately constant. Second, ΔC_{El} is dominated by the w^{-1} noise term rather than the C_{El} sample variance term. The cross-correlation power spectrum C_{Cl} varies more slowly (than linear) with τ and hence $\sigma_C(\tau)$ increases with τ.

Figure 1 also includes the constraint that the optical depth not exceed $\tau_{\rm max}$ calculated as outlined in Section 4. The effect of this $\tau_{\rm max}$ cut is to exclude some of the large optical depth, $\tau \gtrsim 0.2$, models. Without the $\tau_{\rm max}$ cut, the 1-σ contours extend to about $\tau = 0.3$ for $\sigma_E(\tau)$ (and $\tau = 0.25$ for $\sigma_C(\tau)$). With the cut, both the 1-σ contours are restricted to $\tau < 0.2$. As mentioned in Section 4 the parameters we use in our semi-analytical model to calculate $\tau_{\rm max}$ are very conservative. If the optical depth is in fact large, then reionization models will provide significant complementary constraints.

One can look at the detectability of the signal in another way. Let's denote the value of the maximum $C_{E,l}$ for l be-

tween 2 and 20 by $C_{l,\rm peak}$. One can then include $C_{l,\rm peak}$ as a chain parameter and obtain its probability distribution. A rough estimate of the detectability of the signal can be obtained from looking at if $C_{l,\rm peak}$ (signal) is larger than the detector noise contribution; for MAP this noise contribution is $w^{-1} = 5 \times 10^{-15}$.

The distribution of $C_{l,\rm peak}$ peaks at 5.7×10^{-15}. 90% of the models with $z_e > 6.3$ in the chain have $C_{l,\rm peak} > 5.5 \times 10^{-15}$, which tells us that its likely MAP will detect the reionization feature. If we now apply the $\tau_{\rm max}$ cut, then $C_{l,\rm peak} > 4.9 \times 10^{-15}$ for 90% of the models. If we further restrict z_e to between 6.3 and 7, then 90% of the models have $C_{l,\rm peak} > 3.2 \times 10^{-15}$.

We end this section by noting that since A_τ will be determined with very high precision by MAP, the uncertainty in A will be dominated by the uncertainty in τ. If MAP detects the reionization feature as discussed above, then the uncertainty in A is expected to be $\sigma(\ln A) = 2\sigma(\tau) = 0.04$ to 0.06. Note that this is far better than what can be achieved using large angle temperature anisotropy (COBE) data.

6. IS A GRADUAL TRANSITION DISTINGUISHABLE FROM INSTANTANEOUS?

The answer to this question depends on the details of how reionization took place. For simplicity, here we assume a two–step reionization process. We assume that at some $z_{\rm e} > z_{\rm H} = 6.3$, the universe was partially ionized, the ionized fraction being $x_e \leq 1.08$. At around $z = 6.3$, new sources turned on, leading to almost complete ionization. If reionization happened gradually (and not in our idealized two–step fashion) then x_e provides us with an estimate of the average ionized fraction before $z = 6.3$, and z_e an estimate of when the first ionizing sources turned on. As discussed above, the large–scale polarization anisotropy should be insensitive to the topology of the partially ionized regions.

The power spectra used in the analyses described in this section were calculated using the publicly available CMBfast code (Seljak & Zaldarriaga, 1996) which we modified to take into account the two-step reionization process.

We push the arguments outlined in Section 4, to its limit, and assume a minimum virial temperature of 100 K for halos to cool (via H_2 molecules; see Haiman et al., 2000) and form astrophysical objects that can contribute to reionization. Note that gas colder than 100 K can not form H_2 and cool, and therefore can not contract or fragment in the dark halo. We find that this cooling cutoff leads to the result: $z_e \lesssim 40$. In order to have z_e exceed this value, the presence of non-gaussianity in the primordial power spectrum would be required.

Figure 2 shows the effect of different reionization histories. The polarization "bump" due to reionization is unmistakable, as is the lack of power in the model with no reionization (solid curve). The $\exp(-2\tau)$ suppression at large l is not very evident because of the logarithmic scale for the E mode polarization spectrum in panel (a). Note that the variable related to cross-polarization plotted in panel (b) is the coefficient of correlation $r_l = C_{Cl}/\sqrt{C_{El}C_{Tl}}$ (de Oliveira-Costa et al., 2002).

The curves to compare in Figure 2 are the dot-dashed and dotted ones. Both the curves have $\tau = 0.1$; the dotted

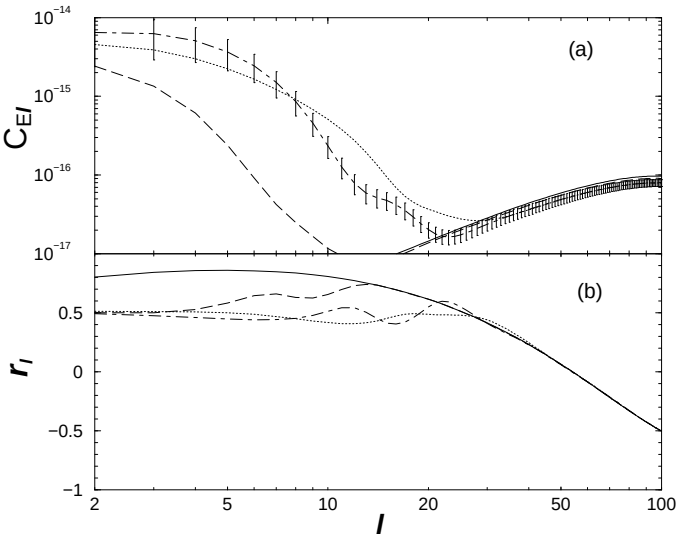

FIG. 2.— Effect of different reionization histories on the CMB anisotropy. Panel (a) shows C_{El}, and (b) shows $r_l = C_{Cl}/\sqrt{C_{El}C_{Tl}}$. Both panels have the same set of reionization histories. The solid curve shows the result of no reionization. The other 3 curves have $z_{\rm H} = 6.3$. The dashed curve has $x_e = 0$ which implies $\tau = 0.033$ (note that x_e is the ionized fraction for $z > z_{\rm H}$). The dotted curve has $\tau = 0.1$ and $z_e = 30$ which requires $x_e = 0.26$. The dot-dashed curve has $\tau = 0.1$ and $z_e = 15$ which requires $x_e = 0.89$. We have added cosmic variance error bars to the $z_e = 15$ C_{El} (dot-dashed) curve.

curve has $z_e = 15$ while the dot-dashed curve has $z_e = 30$. The main effect of increasing z_e at fixed τ is to spread the total reionization–induced power over a larger range of l. In fact, when z_e and z_H are well separated, two reionization "bumps" can be discerned. These are directly related to the bimodal nature of the visibility function for our 2-step reionzation process. The change in the shape of the polarization power spectra due to partial reionzation at $z > z_H$ allows two models with the same optical depth but different reionization histories to be distinguished from each other. For reference we have plotted the cosmic variance error bars given by $\sqrt{2/(2l+1)}C_{E,l}$ for the $z_e = 15$ $C_{E,l}$ curve.

An interesting question, which is part of our broader goal of distinguishing between models with differing ionized fractions beyond $z = 6.3$, is whether one can distinguish a completely neutral hydrogen content at $z > 6.3$ from a partially ionized one. We outline the method used to compare models with different reionization histories below.

Given the spherical harmonic coefficients a^X_{lm} derived from data, one can write down the likelihood function for a particular model (C_{Xl}) given the data as:

$$-2\ln(\mathcal{L}) = \sum_l (2l+1) f_{\rm sky} \Bigg[\ln\left([C_{El} + w^{-1}]\, C_{Tl} - C^2_{Cl} \right) + \frac{[C_{El} + w^{-1}]\, C^d_{Tl} + C_{Tl}\, C^d_{El} - 2C_{Cl}\, C^d_{Cl}}{[C_{El} + w^{-1}]\, C_{Tl} - C^2_{Cl}} \Bigg] \quad (5)$$

where $C^d_{Xl} \equiv \sum_m |a^X_{lm}|^2/(2l+1)$. Eq. 5 was derived under the assumption that a^X_{lm} are gaussian distributed with mean zero. We have set the damping due to the finite experimental beam width to be unity (since we are

only interested in the low l region), and omitted the noise term for C_{Tl} (since it's negligible in comparison to C_{Tl}). We have no data in hand. Instead, we will assume that C^d_{Xl} is given by some fiducial model, $C^{\rm fid}_{Xl}$ (in other words we perform an ensemble average over $\ln(\mathcal{L})$), such that $C^d_{Xl} = C^{\rm fid}_{Xl} + w_X^{-1}$ with $w_C^{-1} = 0$. We then look at the likelihood of other models in this parameter space. Note that all the discriminatory power comes from $l \lesssim 30$. In this regime (as we have shown in Eq. 2) the only cosmological parameters the spectra are sensitive to are the amplitude of power spectrum, tilt and the optical depth.

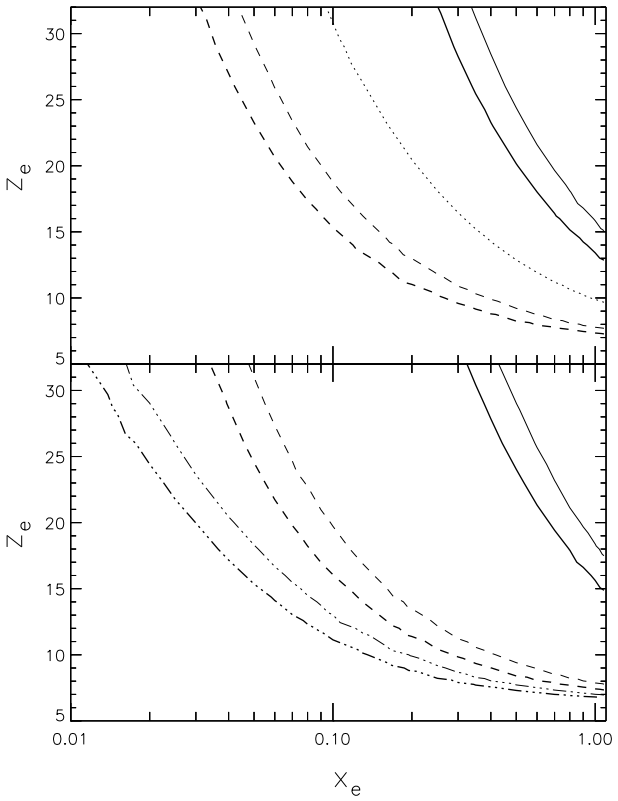

FIG. 3.— Constant likelihood contours at 10% (thick curves) and 1% (thin curves) of the maximum likelihood. The maximum likelihood occurs at the fiducial model, which for this plot is one with no ionized hydrogen at $z > 6.3$. The upper panel assumes two MAP and Planck channels as described in the text. The lower panel assumes one channel per experiment. The solid curves are for MAP. The dashed curves are for Planck. The dot-dashed curves are for a hypothetical SuperPlanck (described in the text). The dotted curve is a constant $\tau = 0.06$ contour.

To fix the amplitude we again use the fact that the CMB constrains the combination $A_\tau = A\exp(-2\tau)$ very well – to about 10% (at 1-σ) with present data (without including massive neutrinos). This will greatly improve with MAP. Note that this particular combination of the amplitude of the power spectrum and optical depth is not affected by the tensor contribution to the anisotropy since the constraints come from the small angular scales. The error in A_τ when propagated to the C_ls is much smaller than cosmic variance on the scales that we consider ($l < 30$). This is simple to see: since the C_ls scale linearly with A, for

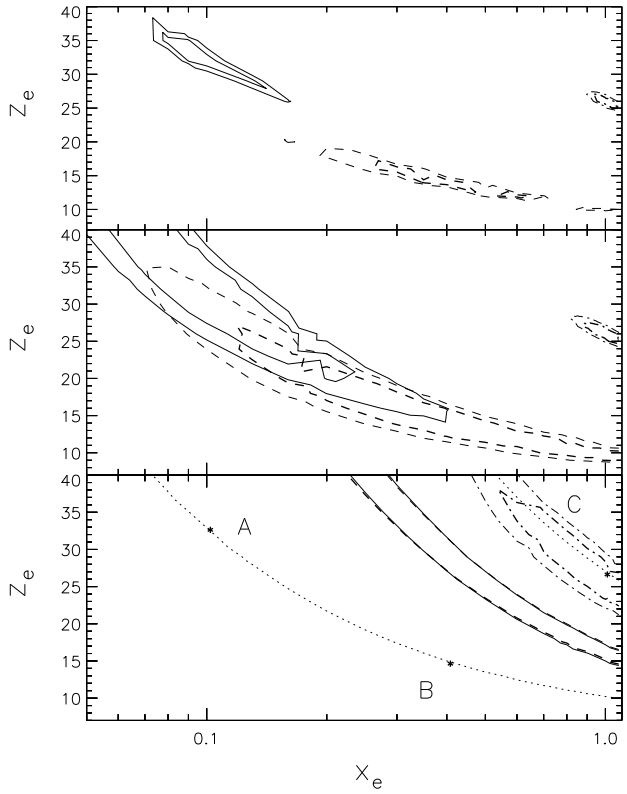

FIG. 4.— Constant likelihood contours at 10% (thick curves) and 1% (thin curves) of the maximum likelihood – which occurs at the fiducial models labeled by A, B and C and denoted by asterisks. A has $z_e = 32$ and $x_e = 0.1$; B has $z_e = 14$ and $x_e = 0.4$; C has $z_e = 26$ and $x_e = 1.0$. All the panels have the same fiducial models. The solid curves correspond to model A, the dashed curves to model B and the dot-dashed curves to model C. The upper panel is for a cosmic variance limited experiment, "SuperPlanck" (see text for details). The middle panel assumes 1 Planck channel sensitivity while the lower panel is for two channel MAP sensitivity. The dotted curves in the lower panel are curves of constant τ for $\tau = 0.063$ and $\tau = 0.25$.

any given τ the fractional theoretical error in C_{Xl} due to the uncertainty in A_τ is $\sigma(A_\tau)/A_\tau$. Thus even with current data this fractional error becomes larger than cosmic variance only at $l > 100$ – safely outside the regime we are interested in.

We set the tilt to unity. Future CMB data sets will determine the tilt well – the expected errors are $\sigma(n) = 0.05$ for MAP and $\sigma(n) = 0.02$ for Planck (allowing for small variations of the spectral index with scale) (Eisenstein et al., 1999). Relaxing this constraint will not affect our results. For C_{El} and C_{Cl}, the predominant effect of tilt (at small l) is just a rescaling of the spectra – degenerate with the amplitude of the power spectrum. The fractional change in $C_{C,El}$ due to a non-zero $n-1$ is $\simeq 4.5(n-1)$. Given the l-range of the signal and the precision with which n will be determined, this is not an issue.

The experiments we consider here are MAP and Planck. To be conservative, as mentioned, we only assume a maximum of two MAP or Planck channels. The best guess at the two relatively foreground–free Planck channels are the

143 and 100 GHz channels (Tegmark et al., 2000). The weight–per–solid angle (for polarization measurements) of the 143 GHz channel for one year of observation is expected to be 1.35×10^{16} and from combining the 100 and 143 GHz channels it's expected that $w = 1.67 \times 10^{16}$.

We will not consider here the balloon borne and terrestrial polarization experiments since these experiments will not have the required sky coverage to obtain spectra at the large angular scales at which reionization imprints its signal.

Figure 3 shows constant likelihood contours for the case where the fiducial model has only neutral hydrogen at $z > 6.3$. The constant likelihood contours are drawn at 10% and 1% of the maximum likelihood. We have considered two separate cases plotted in the upper and lower panels corresponding to sensitivities equal to that of MAP and Planck assuming two channels or a single channel. This is important for MAP since each channel has equal weight.

In the lower panel of Figure 3 we also plot the results for an experiment we dub "SuperPlanck" with a sensitivity which is 25 times better than Planck, i.e., $w = 3.4 \times 10^{17}$. For reference, the raw sensitivity $(1/\sqrt{w})$ of Planck is a factor of 11.6 better than MAP. Clearly, the results of using SuperPlanck are remarkable. We have chosen SuperPlanck to be 25 times more sensitive than Planck because that makes SuperPlanck nearly cosmic variance limited for $z_e < 30$. We study the results of Figure 3 in more detail below.

Let us first concentrate on MAP. Using the 10% likelihood contours, we see that MAP should be able to distinguish a completely neutral hydrogen content at $z > 6.3$ from a case where hydrogen is 50% ionized between the redshifts of $z_{\rm H} = 6.3$ and $z_e = 20$. We see that in this region of parameter space the contours are essentially parallel to the constant τ contours – implying there is very little information except for the value of τ itself.

Planck, of course, can do a much better job. Planck can distinguish between 10% ionized fraction between $z_{\rm H}$ and $z_e = 15$ and the fiducial model which has $x_e = 0$ at $z > z_{\rm H} = 6.3$. The hypothetical SuperPlanck could distinguish the fiducial abrupt–reionization model from one in which $x_e = 0.05$ between $z_{\rm H}$ and $z_e = 15$.

We note that if the universe was indeed reionized close to $z = 6.3$, then MAP will be able to show that $z_e < 13,\ 15$ at 2, 3-σ. Clearly, this will not be sufficient to show that the universe was really abruptly reionized close to $z = 6.3$. However, for the same assumptions, the upper bound from Planck will be $z_e < 7.5,\ 8$. This will be a strong indication that most of the reionization took place close to $z = 6.3$, although delays of $\Delta z \simeq 1$ will still remain a possibility. These results can be read off from Figure 3 (the 10% and 1% contours projected to the $x_e = 1$ line aproximately give the 2 and 3 σ bounds), or derived from Figure 1. From Figure 1 we see that $\sigma(\tau) \simeq 0.025$ (for MAP) which implies $\sigma(z_e) \simeq (2/3) z_e \sigma(\tau)/\tau = 3$ for $z_e = 6.3$. If we assume that both MAP and Planck are noise (and not cosmic variance) limited for $z_e = 6.3$, then we have $\sigma(z_e) \simeq 0.4$ for Planck. This is somewhat better than what Figure 3 implies because cosmic variance is not completely negligible.

One could also ask the following question: if the real universe was completely reionized at some $z > 6.3$, then at what z does it become possible to be certain (say at 3-σ) that $z_e > 6.3$? We can use the discussion of the previous paragraph to answer this question. Taking $\tau \simeq 0.002 z^{1.5}$, we have that $\sigma(z_e) \simeq 333 \sigma(\tau)/\sqrt{z_e}$ and to a good approximation we can assume that $\sigma(\tau)$ is independent of τ for the optical depths we are considering here. Thus if the universe was reionized at a redshift of 13 (8), then MAP (Planck) will be able to claim that $z_e > 6.3$ at the 3-σ level.

We take the above discussion to its natural conclusion by answering the following question: what information can one obtain if the universe is partially ionized at $z > 6.3$? Figure 4 is similar to Figure 3 except we now plot likelihood contours for different fiducial models. Specifically we consider 3 fiducial models: (A) $z_e = 32$ and $x_e = 0.1$, (B) $z_e = 14$ and $x_e = 0.4$, (C) $z_e = 26$ and $x_e = 1.0$. Models (A) and (B) have the same optical depth of $\tau = 0.065$, while model (C) has a large optical depth of $\tau = 0.25$. We see that at the larger optical depth, MAP is sensitive to more than just τ. The distribution of power in l which is decided by z_e is sufficiently different that the contour does not follow the constant τ contour along the entire parameter space. For Planck this happens at the much lower τ of 0.065. It is clear from the Planck contours (upper panel) that cases (A) and (B) can be distinguished despite their equal optical depths.

This is an interesting result. It opens up the possibility that we can observationally determine the reionization history of the universe. The usefulness of such data will be directly determined by the sophistication of the physical modeling of the end dark ages is. We end this section with the tantalizing suggestion that with SuperPlanck, it should be possible to map the evolution of the ionized hydrogen fraction $x_e(z)$ by breaking up the $z_{\rm H}$–z_e redshift interval into several bins and tracing the evolution of x_e.

7. CONCLUSIONS

The remarkable discovery of Gunn-Peterson trough in the spectrum of the redshift $z = 6.28$ quasar has brought into sharp focus the questions of how and when the universe was reionized. While representing a significant new discovery, the power of the hydrogen Gunn–Peterson trough to probe the dark age is limited, because a small neutral hydrogen fraction ($x_{\rm H} \sim 10^{-3}$) is enough to give rise to such a trough. CMB polarization is the most promising way to probe deeper into the dark age; our goal in this paper has been to quantify this statement for forthcoming CMB anisotropy experiments.

Contaminating astrophysical (foreground) sources of polarization may be present at significant levels, but there is very little we know about them. In deriving our results, we have used a maximum of two channels per experiment, with the remainder assumed to be used as foreground monitors. Foregrounds might be more detrimental than we have assumed; the only way to find out is to do multi–frequency CMB experiments.

Using current data we have shown that MAP will most likely detect the reionization feature in the polarization data. We have shown that MAP can measure the electron optical depth to 0.02-0.03 (1-σ), regardless of the value of the optical depth and that this measurement is sufficient to break the degeneracy between the optical depth and

the amplitude of primordial density perturbations. Further, MAP (with two years of observation) will be able to distinguish a model with only neutral hydrogen at $z > 6.3$ from one that was about 50% ionized between $z = 6.3$ and 20. Planck, with its much higher projected sensitivity (and one year of observation), will be able to distinguish an ionized hydrogen fraction of about 6% between the redshifts of 6.3 and 20 from the model with no ionized hydrogen at $z > 6.3$. More strikingly, Planck (and MAP if the optical depth is larger than about 0.2) should be able to differentiate among reionization histories which lead to the *same* optical depth for CMB photons. These results will enormously deepen our understanding of the physics of reionization.

ZH was supported by NASA through the Hubble Fellowship grant HF-01119.01-99A, awarded by the Space Telescope Science Institute, which is operated by the Association of Universities for Research in Astronomy, Inc., for NASA under contract NAS 5-26555. LK and MK were supported by NASA grant NAG5-11098. GPH was supported by W.M. Keck foundation. We thank Uros Seljak and Matias Zaldarriaga for the use of their CMBFAST code.

REFERENCES

Abel, T., Bryan, G. L., & Norman, M. L. 2000, ApJ, 540, 39
Barkana, R. & Loeb, A. 2001, Physics Reports, 349, 125
—. 2002, astro-ph/0204139, submitted to ApJ
Basko, M. M. & Polnarev, A. G. 1980, Mon.Not.Roy.As.Soc., 191, 207
Becker, R. H., Fan, X., White, R. L., Strauss, M. A., Narayanan, V. K., Lupton, R. H., Gunn, J. E., Annis, J., Bahcall, N. A., Brinkmann, J., Connolly, A. J., Csabai, I. ., Czarapata, P. C., Doi, M., Heckman, T. M., Hennessy, G. S., Ivezić, Ž., Knapp, G. R., Lamb, D. Q., McKay, T. A., Munn, J. A., Nash, T., Nichol, R., Pier, J. R., Richards, G. T., Schneider, D. P., Stoughton, C., Szalay, A. S., Thakar, A. R., & York, D. G. 2001, Astron. J., 122, 2850
Bennett, C. L., Banday, A. J., Gorski, K. M., Hinshaw, G., Jackson, P., Keegstra, P., Kogut, A., Smoot, G. F., Wilkinson, D. T., & Wright, E. L. 1996, Astrophys. J. Lett., 464, L1
Bond, J. R., Jaffe, A. H., & Knox, L. 2000, ApJ, 533, 19
Bromm, V., Kudritzki, R. P., & Loeb, A. 2001, ApJ, 552, 464
Carilli, C., Gnedin, N. Y., & Owen, F. 2002, ApJ, in press
Cen, R. & McDonald, P. 2002, ApJ, 570, 457
Christensen, N., Meyer, R., Knox, L., & Luey, B. 2001, Classical Quantum Gravity, 18, 2677
Ciardi, B., Ferrara, A., Governato, F., & Jenkins, A. 2000, Mon.Not.Roy.As.Soc., 314, 611
de Oliveira-Costa, A., Tegmark, M., Zaldarriaga, M., Barkats, D., Gundersen, J. O., Hedman, M. M., Staggs, S. T., & Winstein, B. 2002, astro-ph/0204021
Eisenstein, D. J., Hu, W., & Tegmark, M. 1999, ApJ, 518, 2
Fan, X., Narayanan, V. K., Strauss, M. A., White, R. L., Becker, R. H., Pentericci, L., & Rix, H. 2002, Astron. J., 123, 1247
Furlanetto, S. & Loeb, A. 2002, ApJ, in press, astro-ph/0206308
Gendin, N. Y. 2002, astro-ph/0110290
Gnedin, N. 1999, in ASP Conf. Ser. 193: The Hy-Redshift Universe: Galaxy Formation and Evolution at High Redshift, 598
Gnedin, N. Y. 2000, ApJ, 535, 530
Gnedin, N. Y. & Ostriker, J. P. 1997, ApJ, 486, 581
Gnedin, N. Y. & Ostriker, J. P. 1998, in Structure et Evolution du Milieu Inter-Galactique Revele par Raies D'Absorption dans le Spectre des Quasars, 13th Colloque d'Astrophysique de l'Institut d'Astrophysique de Paris, 33
Gruzinov, A. & Hu, W. 1998, ApJ, 508, 435
Haiman, Z. 2001, in The Mass of Galaxies at Low and High Redshift, Eds. R. Bender and A. Renzini, in press, astro-ph/0112131
Haiman, Z. 2002, ApJ, in press, astro-ph/0205410
Haiman, Z. ., Abel, T., & Madau, P. 2001, ApJ, 551, 599
Haiman, Z. ., Abel, T., & Rees, M. J. 2000, ApJ, 534, 11
Haiman, Z. & Knox, L. 1999, in ASP Conf. Ser. 181: Microwave Foregrounds, 227, astro-ph/9902311
Haiman, Z. & Loeb, A. 1998, ApJ, 503, 505
Halverson, N. W., Leitch, E. M., Pryke, C., Kovac, J., Carlstrom, J. E., Holzapfel, W. L., Dragovan, M., Cartwright, J. K., Mason, B. S., Padin, S., Pearson, T. J., Readhead, A. C. S., & Shepherd, M. C. 2002, ApJ, 568, 38
Hogan, C. J., Kaiser, N., & Rees, M. J. 1982, Royal Society of London Philosophical Transactions Series A, 307, 97
Hogan, C. J. & Rees, M. J. 1979, Mon.Not.Roy.As.Soc., 188, 791
Hu, W. & White, M. 1997, ApJ, 479, 568
Iliev, I. T., Shapiro, P. R., Ferrara, A., & Martel, H. 2002, Astrophys. J. Lett., 572, L123
Kamionkowski, M., Kosowsky, A., & Stebbins, A. 1997, Phys. Rev. Lett., 78, 2058
Kaplinghat, M., Knox, L., & Skordis, C. 2002, ApJ, in press, astro-ph/0203413
Knox, L., Scoccimarro, R., & Dodelson, S. 1998, Phys. Rev. Lett., 81, 2004
Lee, A. T., Ade, P., Balbi, A., Bock, J., Borrill, J., Boscaleri, A., de Bernardis, P., Ferreira, P. G., Hanany, S., Hristov, V. V., Jaffe, A. H., Mauskopf, P. D., Netterfield, C. B., Pascale, E., Rabii, B., Richards, P. L., Smoot, G. F., Stompor, R., Winant, C. D., & Wu, J. H. P. 2001, Astrophys. J. Lett., 561, L1
Leitherer, C., Ferguson, H. C., Heckman, T. M., & Lowenthal, J. D. 1995, Astrophys. J. Lett., 454, L19
Liu, G., Sugiyama, N., Benson, A. J., Lacey, C. G., & Nusser, A. 2001, ApJ, 561, 504
Madau, P., Haardt, F., & Rees, M. J. 1999, ApJ, 514, 648
Miralda-Escudé, J., Haehnelt, M., & Rees, M. J. 2000, ApJ, 530, 1
Nakamoto, T., Umemura, M., & Susa, H. 2001, Mon.Not.Roy.As.Soc., 321, 593
Netterfield, C. B., Ade, P. A. R., Bock, J. J., Bond, J. R., Borrill, J., Boscaleri, A., Coble, K., Contaldi, C. R., Crill, B. P., de Bernardis, P., Farese, P., Ganga, K., Giacometti, M., Hivon, E., Hristov, V. V., Iacoangeli, A., Jaffe, A. H., Jones, W. C., Lange, A. E., Martinis, L., Masi, S., Mason, P., Mauskopf, P. D., Melchiorri, A., Montroy, T., Pascale, E., Piacentini, F., Pogosyan, D., Pongetti, F., Prunet, S., Romeo, G., Ruhl, J. E., & Scaramuzzi, F. 2002, ApJ, 571, 604
Oh, S. P. 1999, in After the Dark Ages: When Galaxies were Young (the Universe at 2 ¡ z ¡ 5). 9th Annual October Astrophysics Conference in Maryland held 12-14 October, 1998. College Park, Maryland. Edited by S. Holt and E. Smith. American Institute of Physics Press, 1999, p. 98, 98, astro-ph/9812318
Oh, S. P. 2001, ApJ, 553, 499
—. 2002, astro-ph/0201517
Oh, S. P. & Haiman, Z. . 2002, ApJ, 569, 558
Pentericci, L., Fan, X., Rix, H., Strauss, M. A., Narayanan, V. K., Richards, G. T., Schneider, D. P., Krolik, J., Heckman, T., Brinkmann, J., Lamb, D. Q., & Szokoly, G. P. 2002, Astron. J., 123, 2151
Press, W. H. & Schechter, P. 1974, ApJ, 187, 425
Prunet, S., Sethi, S. K., & Bouchet, F. R. 2000, Mon.Not.Roy.As.Soc., 314, 348
Rhoads, J. E. & Malhotra, S. 2001, American Astronomical Society Meeting, 199, 0
Seljak, U. & Zaldarriaga, M. 1996, ApJ, 469, 437
Songaila, A. & Cowie, L. L. 2002, Astron. J., 123, 2183
Steidel, C. C., Pettini, M., & Adelberger, K. L. 2001, ApJ, 546, 665
Tegmark, M., Eisenstein, D. J., Hu, W., & de Oliveira-Costa, A. 2000, ApJ, 530, 133
Tozzi, P., Madau, P., Meiksin, A., & Rees, M. J. 2000, ApJ, 528, 597
Tumlinson, J. & Shull, J. M. 2000, Astrophys. J. Lett., 528, L65
Venkatesan, A. 2000, ApJ, 537, 55
—. 2002, ApJ, 572, 15
Venkatesan, A., Giroux, M. L., & Shull, J. M. 2001, ApJ, 563, 1
Wang, Y., Spergel, D. N., & Strauss, M. A. 1999, ApJ, 510, 20
Zaldarriaga, M. 1997, Phys. Rev., D55, 1822
Zaldarriaga, M. & Seljak, U. 1997, Phys. Rev., D55, 1830
Zaldarriaga, M., Spergel, D. N., & Seljak, U. 1997, ApJ, 488, 1